Morphology of Diblock Copolymers of Norbornene and Organometallic Derivatives of Norbornene

V. Sankaran,† R. E. Cohen,*,† C. C. Cummins,‡ and R. R. Schrock‡

Departments of Chemical Engineering and Chemistry, Massachusetts Institute of Technology, Cambridge, Massachusetts 02139

Received July 2, 1991

ABSTRACT: Diblock copolymers of norbornene and an organometallic derivative of norbornene, Sn[2,3-*trans*-bis[(*tert*-butylamido)methyl]norborn-5-ene]Cl_2, were synthesized via ring-opening metathesis polymerization using a tungsten alkylidene catalyst. The morphologies of these copolymers were investigated by transmission electron microscopy (TEM) and small-angle X-ray scattering (SAXS). The copolymers exhibited spherical, cylindrical, or lamellar morphology depending on their composition and molecular weight. The phase diagram compares well with the predictions of the Helfand and Wasserman theory. The interdomain spacing (d) for the spherical and lamellar polymers scales with copolymer molecular weight to the 0.49 power and 0.67 power, respectively. Additionally the SAXS data for two copolymers with spherical morphologies were fitted to a model to obtain information on the size and packing of the organometallic spheres.

Introduction

Several studies in recent years have focused on the size-dependent evolution of properties in nanoscale (diameter ≤ 500 Å) aggregates of metallic and semiconducting materials.[1] These materials exhibit hybrid properties in between the molecular and bulk solid-state limits. As a result of their incompletely developed electronic structures, a regular array of these aggregates or clusters may exhibit novel optical, electronic, and magnetic properties. A major stumbling block in achieving these goals has been the inability to synthesize monodisperse clusters in significant quantities.

In a recent paper[2] we outlined a new technique to synthesize semiconductor clusters. Our technique takes advantage of the uniform microdomain structure resulting from the self-assembling nature of block copolymers.[3] Synthesis of a diblock copolymer of norbornene and an organometallic monomer allows for the transport of metal atoms into the block copolymer microdomains, inside which clusters can be grown in a controlled fashion. In a subsequent paper[4] we reported the synthesis of two new ligands bTAN [2,3-*trans*-bis[(*tert*-butylamido)methyl]-norborn-5-ene] and bSAN [2,3-*trans*-bis[[(trimethylsilyl)amido]methyl]norborn-5-ene] for the preparation of organometallic monomers, characterization of a tin monomer [Sn(bTAN)Cl_2, **1**] prepared using the bTAN ligand, and results for the polymerization of monomer **1** by well-characterized ring-opening metathesis polymerization (ROMP) initiators such as M(CH^{t}Bu)(NAr)(O^{t}Bu)$_2$ [M = W or Mo and Ar = 2,6-^{i}Pr$_2$C$_6$H$_3$]. Also included was the characterization by transmission electron microscopy (TEM) of a 50/50 wt % polynorbornene/poly-**1** diblock of 11 500 molecular weight exhibiting lamellar morphology.

Here we report the results of a detailed structural characterization of the same polynorbornene/poly-**1** system. A series of copolymers has been studied by gel permeation chromatography (GPC), TEM, and small-angle X-ray scattering (SAXS). Results are presented in the form of a phase diagram relating morphology to copolymer molecular weight and relative block lengths. The scaling of interdomain spacing as a function of the copolymer molecular weight was studied for polymers with spherical and lamellar morphologies. The results were compared to the predictions of the microphase-separation theory developed by Helfand and Wasserman.[5] Additionally quantitative information on domain size and packing was obtained from SAXS data for the samples exhibiting spherical morphology.

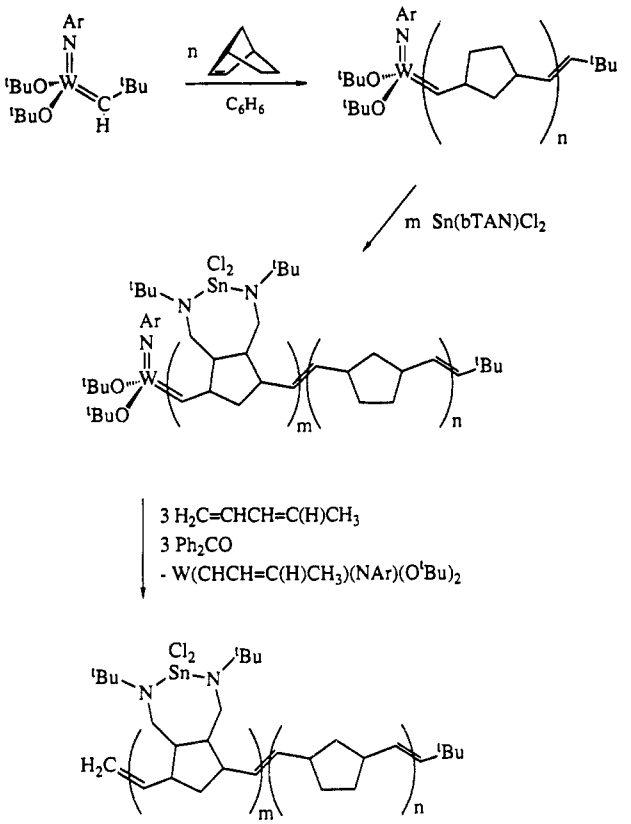

Figure 1. Schematic for the synthesis of polynorbornene/poly-**1** diblock copolymers via ROMP.

Experimental Section

Chemicals and Reagents. All reactions were performed in a Vacuum Atmospheres nitrogen glovebox. All glassware used was flame dried under vacuum. Benzene was vacuum distilled from a flask containing sodium sand, stored over Na/K alloy, and filtered through a sintered-glass frit prior to use. Norbornene was distilled from molten sodium under a slight overpressure of argon. W(CH^{t}Bu)(NAr)(O^{t}Bu)$_2$ [Ar = 2,6-^{i}Pr$_2$C$_6$H$_3$)] and monomer **1** were synthesized as described in the literature.[4,6]

† Department of Chemical Engineering.
‡ Department of Chemistry.

0024-9297/91/2224-6664$02.50/0

Table I
Summary of the Characterization of the Different Block Copolymers Synthesized

sample ID	exptd mol wt ($M_w \times 10^{-3}$) (polynorbornene/poly-1)	obsd mol wt (M_w) of polynorbornene block (PDI)[a]	calcd mol wt (M_w) of poly-1 block[b]	wt fraction of poly-1 block	morphology (TEM)
A	111/16	111 300 (1.30)	15 800	0.13	spherical
B	21/21	21 400 (1.05)[c]	21 500	0.50	lamellar
C	19/9	21 200 (1.04)	10 200	0.33	cylindrical
D	8/8	7 900 (1.06)	7 800	0.50	lamellar
E	11/11	11 500 (1.08)	11 500	0.50	lamellar
F	47/7	52 000 (1.04)[d]	7 500	0.13	spherical
G	23.5/3.5	26 200 (1.05)	3 800	0.13	spherical
H	4.1/4.1	5 100 (1.07)	5 200	0.50	lamellar
I	141/20	190 600 (1.33)	27 600	0.13	spherical
J	70.5/10	79 300 (1.06)[d]	11 300	0.13	spherical
K	47/47	54 500 (1.03)	54 300	0.50	lamellar

[a] Molecular weights determined by GPC. Values reported were obtained by dividing the equivalent PS molecular weight by 2. PDI indicates polydispersity index, i.e., M_w/M_n. [b] Molecular weights reported based on first block molecular weights and on the assumptions of termination-free crossover and 100% conversion of monomer 1. [c] Sample had ~10 wt % of high molecular weight polymer (M_w = 581 100 with PDI = 1.43). [d] Osmometry yielded M_n values of 51 100 for sample F and 67 500 for sample J.

Polymerization Chemistry. Block copolymers of norbornene and 1 were synthesized by sequential addition of the monomers to W(CH^{t}Bu)(NAr)(O^{t}Bu)$_2$ in benzene, with the norbornene block being polymerized first (Figure 1). ROMP initiators are usually terminated using aldehydes such as benzaldehyde or pivaldehyde. However, NMR experiments indicated that monomer 1 (most likely the Sn atom) reacts rapidly with aldehydes giving a complex mixture of products. We therefore terminated the polymerization by the addition of *trans*-1,3-pentadiene which reacts rapidly with the living polymer yielding a vinyl-terminated polymer and a new alkylidene which is then terminated over a period of time by reaction with benzophenone. Control NMR experiments confirmed that 1 is unreactive toward *trans*-1,3-pentadiene and benzophenone.

The following conditions are used to prepare a 200/20 diblock copolymer of polynorbornene/poly-1. A solution of 15 mg (2.6×10^{-5} mol) of catalyst in 1.5 mL of benzene was added to a stirring solution of 490 mg (5.2×10^{-3} mol) of norbornene in 15.5 mL of benzene. After 10 min, 2 mL of the reaction mixture was withdrawn using a pipette and terminated with benzaldehyde. This aliquot was used to obtain a GPC trace of the first block. A solution of 208 mg (4.6×10^{-4} mol) of monomer 1 in 5 mL of benzene was then added to the reaction mixture. After 20 min 9.17 μL (1×10^{-4} mol) of pentadiene and 16.76 mg (1×10^{-4} mol) of benzophenone were added to terminate the reaction. The reaction was allowed to stir for another 1 h to ensure complete termination. Other polymers were prepared by appropriately changing the relative amounts of monomers added.

Molecular Weight Characterization. Molecular weights were obtained using a GPC setup comprised of four μ-Styragel columns (500, 10^2, 10^3, and 10^4 Å) in series followed by a refractive index detector and a UV/vis detector. The solvent was dichloromethane at a flow rate of 1.00 mL/min. The sample volume injected was 100 μL, and the concentration of polymer in the sample was ~0.2 wt %. Number-average molecular weights were determined by osmometry using a Wescan recording osmometer Model 231. The solvent was toluene, and the membrane used had a molecular weight cutoff of about 15 000.

Density Measurements. The density of polynorbornene was determined using a density gradient column composed of ethanol, water, and sodium chloride. The column was calibrated using glass floats of densities 0.8511, 0.8984, 0.9546, and 1.004 g/cm^3. To estimate the density of poly-1, we used a sink–float method with halogenated alkane liquids of varying densities.

Morphological Characterization. Films were solution cast directly from the polymerization mixture inside the nitrogen drybox. The polymerization mixture was transferred to a Teflon-lined cup placed inside a sealed glass jar (diameter = 7 cm; height = 7 cm). The cap of the jar had four holes of 1-mm diameter. The solvent (benzene) was allowed to evaporate slowly over 5–8 days to obtain a transparent yellow film, which was further dried under vacuum for 24 h. SAXS experiments were performed using a Rigaku instrument with a 1.54-Å Cu Kα rotating-anode point source, Charles Supper double-mirror-focusing optics, and a Nicolet two-dimensional detector. The setup was calibrated using cholesteryl myristate [long period (d) = 50.7 Å].[7]

Ultrathin sections obtained using a LKB Ultratome III Model 8800 were studied by transmission electron microscopy (Jeol CX-200, operating voltage 200 kV, and Philips EM300, operating voltage 100 kV). The X-ray fluorescence experiment was performed on a STEM (VG-HB5, operating voltage 100 kV). EM300 was calibrated against a diffraction-grating carbon replica (21 600 lines/cm).

Results

Block copolymers of norbornene and 1 were synthesized with specific block lengths to target a variety of morphologies. The composition of these polymers, their molecular weights, and observed morphologies are summarized in Table I. Molecular weights of the first blocks were obtained by GPC. The diblock itself could not be analyzed by GPC as the Sn–N bond in 1 is readily cleaved by trace amounts of moisture and oxygen. The molecular weight of the second block was obtained from the first block molecular weight and the amount of monomer 1 added with the assumption of termination-free crossover and complete monomer comsumption. The GPC results clearly indicate the synthesis of a low-polydispersity first block with roughly the expected molecular weight. The polynorbornene molecular weights reported were obtained by dividing the equivalent polystyrene molecular weights by a factor of 2. This value of 2 is based on comparison of the stochiometric molecular weight to the polystyrene equivalent molecular weight of a number of norbornene homopolymers prepared over the years in our laboratory. Additional proof comes from osmometry measurements on polynorbornene blocks of samples F and J (M_n = 51 100 for sample F and 67 500 for sample J).

One can clearly observe the microphase-separated morphology of these polymers by TEM. Representative micrographs of the different morphologies observed are shown in Figure 2. The dark areas represent the Sn-containing phase, i.e., poly-1 regions, as confirmed by X-ray fluorescence spectroscopy in a scanning transmission electron microscope (STEM).[8] A density map obtained by monitoring the Sn L signal (3.3–3.9 keV) correlates with the corresponding bright-field STEM micrograph for sample E (Figure 3). The tin therefore acts as an inherent stain, making it very easy to observe morphology in this system. This elegantly solves a major problem faced in studying the morphology of ROMP block copolymers by TEM, as the presence of double bonds in both blocks makes it very difficult to selectively stain one of them.

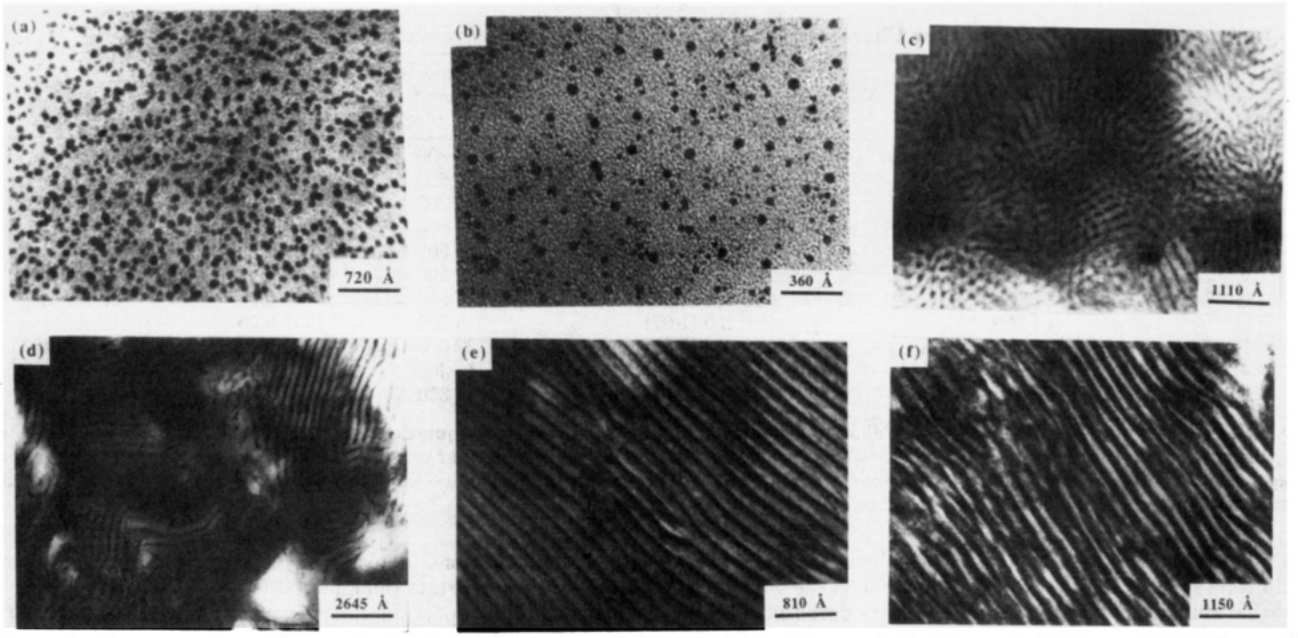

Figure 2. Representative micrographs for the different polymers synthesized: (a) sample A, (b) sample I, (c) sample C, (d) sample B, (e) sample E, (f) sample K.

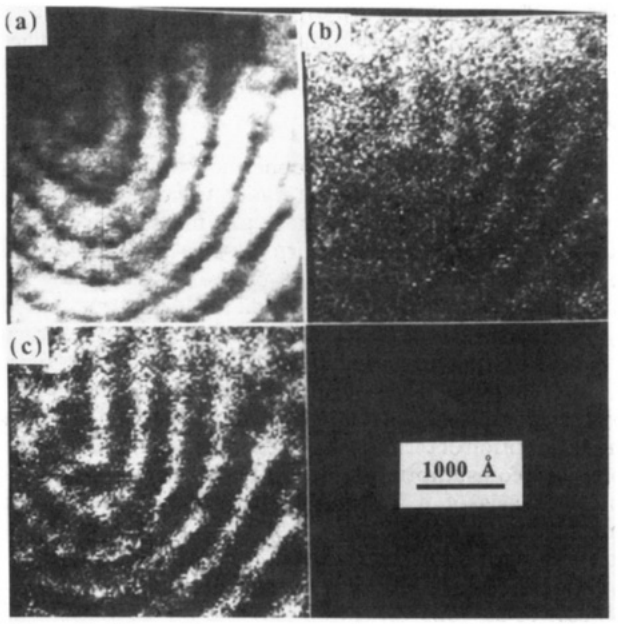

Figure 3. X-ray fluorescence spectroscopy data collected on the STEM for sample E: (a) bright-field micrograph; (b) O pulse map obtained by monitoring the K signal (0.4–0.6 keV); (c) Sn pulse map obtained by monitoring the L signal (3.3–3.9 keV).

TEM samples were microtomed in air, resulting in the hydrolysis of a significant amount of Sn as substantiated by the correspondence between the Sn and O density maps shown in Figure 3. The Sn atoms are no longer covalently bonded to the bTAN ligand, raising questions about their mobility within the heterogeneous polymer morphology. The excellent contrast and sharp boundaries in the Sn map indicate that the hydrolyzed Sn atoms have only limited mobility.

SAXS spectra were obtained by collecting data for 30 min and subtracting out the required background scattering. A typical two-dimensional SAXS pattern is shown in Figure 4a. The two-dimensional SAXS pattern for each of the samples was a clearly discernible ring at a particular value of scattering vector Q, where $Q = (4\pi/\lambda) \sin \theta$, the scattering angle being 2θ. The symmetry in the two-dimensional pattern indicates no preferred large-scale orientation of the morphology and is a consequence of our film preparation technique. Radial-averaged plots of

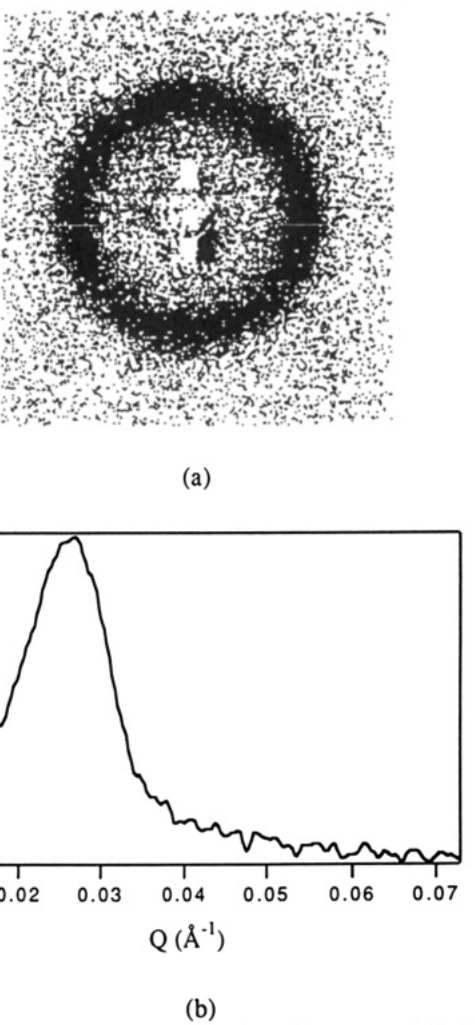

Figure 4. SAXS data for sample D collected over a period of 30 min: (a) two-dimensional pattern after correcting for background scattering; (b) radial-averaged plot of intensity, I (counts), vs scattering vector, Q(Å), obtained from the two-dimensional pattern.

Table II
Morphology and *d* Spacing for the Different Samples

sample ID	morphology	*d* spacing,[a] Å
A	spherical	500
B	lamellar	510
C	cylindrical	340
D	lamellar	240
E	lamellar	300
F	spherical	330
G	spherical	250
H	lamellar	160
I	spherical	660
J	spherical	370
K	lamellar	770

[a] Obtained using SAXS data.

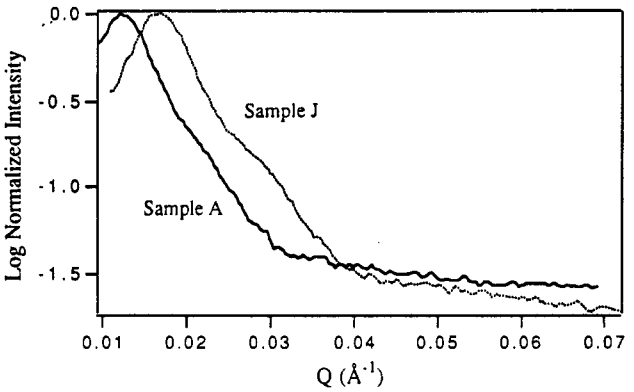

Figure 5. Radial-averaged plots of intensity (I) vs scattering vector (Q) obtained for samples A and J over a period of 2 h. The data have been corrected for background scattering.

intensity (I) as a function of scattering vector (Q) obtained from the SAXS patterns show a single peak in each case [Figure 4b]. The radial-averaged plots were obtained from the two-dimensional pattern by calculating an average intensity around the circumference at each value of Q along the radius. The interdomain spacing ($d = 2\pi/Q_{max}$) for each of the polymers was obtained from the location of the maximum in the I vs Q plot; these morphological distances are listed in Table II. In the case of polymers A and J with spherical morphologies, increasing the collection time to 2 h revealed the presence of a distinct shoulder in the SAXS pattern (Figure 5). The presence of a shoulder instead of resolvable higher order peaks is an indication of a disordered arrangement of spheres.[9]

Qualitatively, results from SAXS and TEM compare well with each other. In both cases we see an absence of any long-range order in any of the copolymers. This lack of order is a result of nonequilibrium effects encountered in the solvent evaporation process[10] (see the Discussion section). Quantitatively we do not have good agreement between our SAXS and TEM results. Interdomain spacings obtained by SAXS are always significantly higher than those obtained by TEM. We note that norbornene, which is the matrix block in all our polymers, has a T_g of 35–45 °C,[11] and because our microtoming is done at room temperature, significant compression of the polymer morphology could occur, resulting in the smaller d spacings observed in TEM. We therefore consider the results obtained by SAXS to be more reliable.

Additional information on domain size and domain packing was obtained by fitting some of our SAXS spectra to models employed earlier[9a,12-15] for more conventional, fully organic diblock copolymers. The analysis was carried out on samples A and J, both of which exhibit spherical morphology. The model includes scattering from two mechanisms: interparticle and intraparticle interference. The intraparticle scattering (f) was described with the Bessel function $J_{3/2}$ as shown below,[9b,12] where R_b is the radius of domains

$$f_{sphere}^2(QR_b) = \frac{9\pi}{2}\left[\frac{J_{3/2}(QR_b)}{(QR_b)^{3/2}}\right]^2 = \left[\frac{3}{(QR_b)^3}\right]^2[\sin(QR_b) - QR_b\cos(QR_b)]^2 \quad (1)$$

The interparticle scattering was modeled as described by Kinning and Thomas[9a] using the closed-form solution for the Percus–Yevick correlation function developed by Wertheim[13] and Thiele.[14] This solution assumes a hard-sphere behavior for the interacting spherical domains. The calculation is expressed in terms of the hard-sphere volume fraction, η, which is defined as

$$\eta = 4/3\pi R_{hs}^3 n \quad (2)$$

where R_{hs} is the effective radius of the hard spheres and n is the number of hard spheres per cubic centimeter. Three other parameters α, β, and γ are defined in terms of η as follows.

$$\alpha = (1 + 2\eta)^2/(1 - \eta)^4 \quad (3)$$

$$\beta = -6\eta(1 + \eta/2)^2/(1 - \eta)^4 \quad (4)$$

$$\gamma = \eta/2(1 + 2\eta)^2/(1 - \eta)^4 \quad (5)$$

As shown by Kinning and Thomas, the interparticle interference factor, S, is written as

$$S(Q,R_{hs},\eta) = \frac{1}{1 + 24\eta(G(A)/A)} \quad (6)$$

where $A = 2QR_{hs}$ and

$$G(A) = \frac{\alpha}{A^2}(\sin A - A\cos A) + \frac{\beta}{A^3}[2A\sin A + (2 - A^2)\cos A - 2] + \frac{\gamma}{A^5}\{-A^4\cos A + 4[(3A^2 - 6)\cos A + (A^3 - 6A)\sin A + 6]\} \quad (7)$$

The total scattering can then be represented as[15]

$$I(Q,R_{hs},R_b) = KS(Q,R_{hs},\eta)f_{sphere}^2(QR_b) + I_{inc} \quad (8)$$

The incoherent scattering (I_{inc}) was essentially zero for our samples. K is the contrast factor, which is the difference in the electron densities of the particle and the matrix. As K for the polynorbornene/poly-1 system is unknown, we compared our calculated and observed spectra after normalizing them with their respective maxima.

Parts a and b of Figure 6 show the results of the calculations described above together with the SAXS spectra for samples A and J. The excellent fit confirms the applicability of the model to organometallic copolymers. The two samples had a η value ~0.28, which implies a poor packing of the spheres (η = 0.74 for fcc and hcp packing and 0.68 for bcc packing[16]). The R_{hs} values obtained were approximately half the d spacing observed by SAXS for these samples. We also found that the position of the shoulder is remarkably sensitive to the value of R_b (Figure 6b). Thus, even though our data exhibit no distinct higher angle peaks, we can determine the value of R_b. We obtained R_b values of 130 and 100 Å for samples A and J, respectively, from our model. These values were approximately twice those obtained by TEM (60 Å for

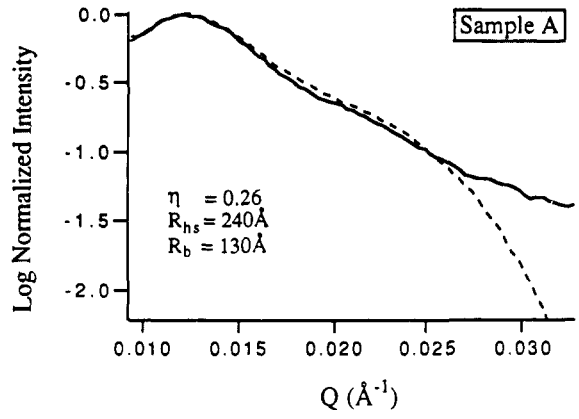

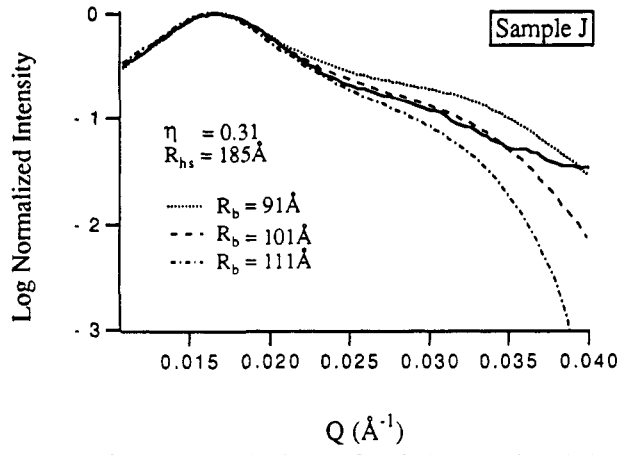

Figure 6. Comparison of calculated and observed SAXS data for samples A and J. The solid line is the observed data and the dashed line the fitted curve.

sample A and 50 Å for sample J). A similar discrepancy in domain sizes obtained from SANS and TEM was observed by Berney et al. for polystyrene/polybutadiene diblock copolymers (SANS results were 1.3 times larger than the TEM results).[17] At present we do not have a definite explanation for this discrepancy. Possible explanations are the compression of the morphology during microtoming or the aggregation of the hydrolyzed Sn atoms within the domains (SAXS experiments use bulk samples in which the Sn atoms may not be significantly hydrolyzed).

Discussion

Typically one can develop a phase diagram representing the morphology of a block copolymer as a function of the total copolymer molecular weight and volume fraction of one of the blocks. Usually volume fractions are replaced by weight fractions, as most organic polymers have densities close to 1. Density measurements yield a value of 0.97 g/cm^3 for polynorbornene and 1.3–1.4 g/cm^3 for poly-1. We therefore present our phase diagram (Figure 7) in terms of volume fractions using an average density of 1.35 for poly-1. Microphase separation occurs at copolymer molecular weights as low as 15 000, implying a large value for the Flory–Huggins interaction parameter (χ) for this system. For a block copolymer with equal volume fractions of the two blocks, microphase separation occurs for $\chi N \geq 10.5$, where N is the degree of polymerization. Similar calculation for this system (based on

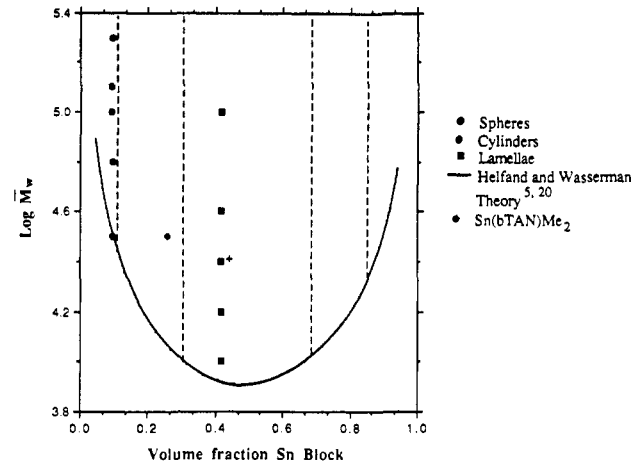

Figure 7. Phase diagram for the polynorbornene/poly-1 system at room temperature (~20 °C). The density of poly[Sn(bTAN)-Me$_2$] has been assumed to be identical to that of poly-1.

sample H) gives $\chi \geq 0.17$, significantly larger than the value of 0.03–0.04 observed for the styrene/butadiene system.[18] This large value observed for χ is remarkable considering that monomer 1 primarily has a polynorbornene backbone. The large positive value of χ is due to the highly polar nature of monomer 1, which in turn is a result of the highly polar Sn–Cl bonds; it does not arise directly from the presence of the metal atom. Replacing the Sn–Cl bonds in 1 by the less polar Sn–Me bonds significantly reduces the χ parameter and increases the minimum molecular weight required for phase separation of polynorbornene/poly-1(methyl derivative) copolymers. A diblock copolymer of norbornene and the Sn–Me derivative of 1 with a copolymer molecular weight of 22 500 and a composition of 52 wt % Sn–Me block is homogeneous (see Figure 7).

The large value of χ for the polynorbornene/poly-1 system puts most of the polymers synthesized in the strong segregation limit,[19] i.e., $\chi N \gg 10.5$. In this limit the most successful microphase-separation theory is the self-consistent mean-field theory proposed by Helfand and Wasserman,[5,20] who developed a free-energy expression for a microphase-separated system and numerically solved it to calculate the phase diagram for polystyrene/polybutadiene. The curve shown in Figure 7 was determined by shifting the Helfand–Wasserman phase diagram vertically to fit our data. The compositions that delineate the thermodynamic stability of different morphologies have also been taken from ref 20 (these boundaries are virtually independent of molecular weight and temperature).

In the strong segregation limit the interdomain spacing (d) scales as $d \sim M^a$, where M is the total copolymer molecular weight. The value of exponent a is predicted to be $^9/_{14}$ (~0.64).[19,20] For block copolymers of styrene/isoprene and styrene/butadiene exhibiting lamellar[21] and spherical[10a] morphology, Hashimoto found the exponent to be $^2/_3$. For our system we found the exponent to be 0.66 and 0.49 for samples having lamellar morphology and spherical morphology, respectively (Figure 8). The deviation from theory exhibited by the spherical samples has been observed previously.[9b,22] This discrepancy was explained by Hashimoto et al.[10,21] as a result of nonequilibrium effects of solvent casting. Experimentally Shibayama et al.[23] found that there is a tendency for domain size to increase as the concentration of the casting solvent decreases. For the case of spherical morphology this can be accomplished only by increasing the number of polymer

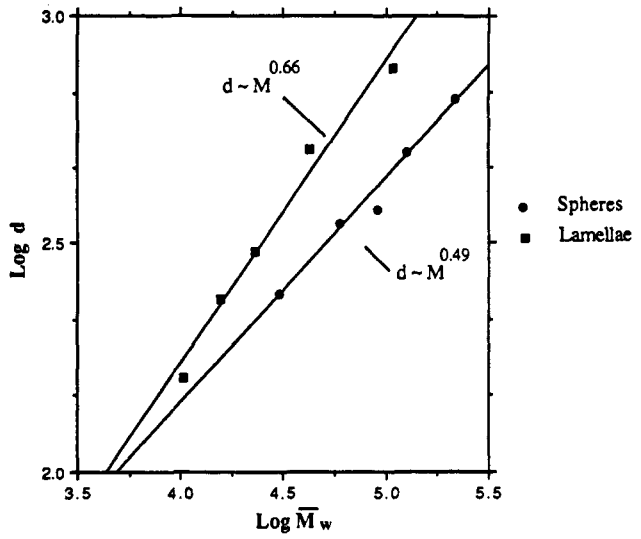

Figure 8. Interdomain spacing, d(Å), as a function of copolymer molecular weight, M_w. The d spacings were determined by SAXS.

chains in each domain. This size increment requires transport of B chains through a matrix of A chains, a process of very high activation energy when the solvent concentration is low. Therefore, the observed spherical domain size in bulk is a manifestation of an equilibrium concentration lower than 100% copolymer, resulting in a smaller than expected domain size and d spacing. As discusssed by Bates et al.[9b] this domain size discrepancy becomes more pronounced at higher molecular weights, thereby leading to a lower than expected slope in the scaling law for the spherical system.

Conclusions

Block copolymers of polynorbornene and organometallic poly-1 exhibit morphologies and scaling laws which can be well understood with the existing framework of theories for wholly organic block copolymers. The present set of observations will enable us to anticipate the morphological behavior of various other block copolymer systems which contain organometallic moieties. With an appropriate phase diagram and scaling laws it should be possible to target a desired morphology and domain size for a selected organometallic system. This would in turn allow us to synthesize metallic or metal-containing clusters of desired size and shape. Currently we are investigating the growth of semiconductor clusters within the microdomains of block copolymers synthesized using Sn(II) and Pb(II) analogues of 1.

Acknowledgment. This research was supported primarily by the MSF/MRL through the Center for Material Science and Engineering at MIT under Grant DMR87-19217.

References and Notes

(1) (a) Andres, R. P.; Averback, R. S.; Brown, W. L.; Brus, L. E.; Goddard, W. A., III; Kaldor, A.; Louie, S. G.; Moscovits, M.; Peercy, P. S.; Riley, S. J.; Siegel, R. W.; Spaepen, F.; Wang, Y. *J. Mater. Res.* **1989**, *4* (3), 704–736. (b) Brus, L. *J. Phys. Chem.* **1986**, *90*, 2555–2560. (c) Yuan, Y.; Cabasso, I.; Fendler, J. H. *Macromolecules* **1990**, *23*, (12), 3198–3200. (d) Wang, Y.; Suna, A.; Mahler, W.; Kasowski, R. *J. Chem. Phys.* **1987**, *87* (12), 7315–7322. (e) Loung, J. C. *Superlattices and Microstructures* **1988**, *4*, (3), 385–390.
(2) Sankaran, V.; Cummins, C. C.; Schrock, R. R.; Cohen, R. E.; Silbey, R. J. *J. Am. Chem. Soc.* **1990**, *112*, 6858–6859.
(3) (a) Leibler, L. *Macromolecules* **1980**, *13*, 1602. (b) Noshay, A.; McGrath, J. E. *Block Copolymers*; Academic Press Inc.: New York, 1977. (c) Sadron, C.; Gallot, B. *Makromol. Chem.* **1973**, *164*, 301–332. (d) Meier, D. J. *J. Polym. Sci, Part C* **1969**, *26*, 81–98.
(4) Cummins, C. C.; Schrock, R. R.; Vale, M. G.; Sankaran, V.; Cohen, R. E., submitted for publication in *Chem. Mater.*
(5) Helfand, E.; Wasserman, Z. R. *Polym. Eng. Sci.* **1977**, *17* (8), 582–586.
(6) Schrock, R. R.; DePue, R. T.; Feldman, J.; Yap. K. B.; Yang, D. C.; Davis, W. M.; Park, L.; DiMare, M.; Schofield, M.; Anhaus, J.; Walborsky, E.; Evitt, E.; Kruger, C.; Betz, P. *Organometallics* **1990**, *9*, 226.
(7) Craven, B. M.; DeTitta, G. T. *J. Chem. Soc., Perkin Trans. 2* **1976**, *7*, 814–822.
(8) Gebizlioglu, O. S.; Cohen, R. E.; Argon, A. S. *Makromol. Chem.* **1986**, *187*, 431–439.
(9) (a) Kinning, D. J.; Thomas, E. L. *Macromolecules* **1984**, *17*, 1712–1718. (b) Bates, F. S.; Berney, C. V.; Cohen, R. E. *Macromolecules* **1983**, *16*, 1101–1108.
(10) (a) Hashimoto, T.; Fujimura, M.; Kawai, H. *Macromolecules* **1980**, *13*, 1660–1669. (b) Cohen, R. E.; Bates, F. S. *J. Polym. Sci.* **1980**, *18* (10), 2143–2148.
(11) (a) Cooper, W. *Eur. Polym. J.* **1975**, *11*, 833. (b) Stein, C.; Marbach, A. *Rev. Gen. Caoutch. Plast.* **1975**, *52* (1–2), 71. (c) Muller, J. C. German Patent 1961742, 1968.
(12) Guinier, A.; Fournet, G. *Small-Angle Scattering of X-Rays*; Wiley: New York, 1955.
(13) Wertheim, M. S. *Phys. Rev. Lett.* **1963**, *10*, 321.
(14) Thiele, E. *J. Chem. Phys.* **1963**, *39*, 474.
(15) Berney, C. V.; Cheng, P. L.; Cohen, R. E. *Macromolecules* **1988**, *21*, 2235–2240.
(16) Atkins, P. W. *Physical Chemistry*, 2nd ed.; W. H. Freeman and Co.: San Fransisco, 1982.
(17) Berney, C. V.; Cohen, R. E.; Bates, F. S. *Polymer* **1982**, *23*, 1222–1226.
(18) Narasimhan, V.; Huang, R. Y. M.; Burns, C. M. *J. Polym. Sci: Polym. Phys. Ed.* **1983**, *21*, 1993–2001.
(19) Bates, F. S.; Fedrickson, G. H. *Annu. Rev. Phys. Chem.* **1990**, *41*, 525.
(20) Helfand, E.; Wasserman, Z. R. In *Developments in Block Copolymers-1*; Goodman, I., Ed.; Applied Science Publishers: New York, 1985; Chapter 4.
(21) (a) Hashimoto, T. *Macromolecules* **1982**, *15*, 1548–1553. (b) Hashimoto, T.; Shibayama, M.; Kawai, H. *Macromolecules* **1980**, *13*, 1237–1247.
(22) (a) Richards, R. W. *Small Angle Neutron Scattering from Block Copolymers. Adv. Polym. Sci.* **1985**, *71*. (b) Mori, K.; Hasegawa, H.; Hashimoto, T. *Polymer* **1990**, *31*, 2368–2376. (c) Shibayama, M.; Hashimoto, T.; Kawai, H. *Macromolecules* **1983**, *16*, 16–28.
(23) Shibayama, M.; Hashimoto, T.; Kawai, H. *Macromolecules* **1983**, *16*, 1434–1443.

Registry No. 1-norbornene (copolymer), 136692-92-7.